Tailored Synthesis of Intelligent Polymer Nanocapsules: An Investigation of Controlled Permeability and pH-Dependent Degradability

Xin Huang,[†,*] Dietmar Appelhans,[†,*] Petr Formanek,[†] Frank Simon,[†] and Brigitte Voit[†,‡]

[†]Leibniz Institute of Polymer Research Dresden, Hohe Strasse 6, 01069 Dresden, Germany and [‡]Organic Chemistry of Polymers, Technische Universität Dresden, 01062 Dresden, Germany

ABSTRACT In this study, we present a new route to synthesize an intelligent polymer nanocapsule with an ultrathin membrane based on surface-initiated reversible addition–fragmentation chain-transfer polymerization. The key concept of our report is to use pH-responsive polydiethylaminoethylmethacrylate as a main membrane-generating component and a degradable disulfide bond to cross-link the membrane. The permeability of membrane, tuned by adjusting pH and using different lengths of the cross-linkers, was proven by showing a dramatic swelling behavior of the nanocapsules with the longest cross-linker from 560 nm at pH 8.0 to 780 nm at pH 4.0. Also, due to the disulfide cross-linker, degradation of the capsules using GSH as reducing agent was achieved which is further significantly promoted at pH 4.0. Using a rather long-chain dithiol cross-linker, the synthesized nanocapsules demonstrated a good permeability allowing that an enzyme myoglobin can be postencapsulated, where the pH controlled enzyme activity by switching membrane permeability was also shown.

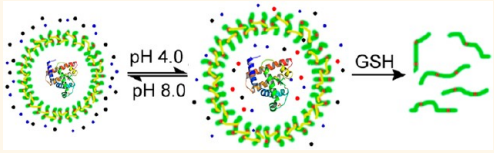

KEYWORDS: polymer nanocapsules · nanoreactor · degradability · pH sensitive · permeability

Presently, it is a high goal of many scientists, dominated by polymer chemists, to create a simple chemical model for studying complex biological systems.[1−3] One of the recent success stories in this field is the ability to tailor the self-assembly of polymers into polymersomes to investigate the control of transmembrane transport in biology.[4−11] Furthermore, these polymersomes can be ideal candidates for artificial cells, nanocarriers, or nanoreactors.[4−11] To fulfill the role in these applications, a fundamental requirement is the presence of a permeable, but also stable membrane which can allow molecules to diffuse in and out of those polymersomes. In comparison with liposomes, the high molecular weight polymer units in polymersomes on the one hand truly enhance mechanical and chemical structure stability. On the other hand, it leads to some extent to loss of permeability and dynamics of the membrane in polymersomes. Up to now, great efforts have been made to improve this.[12−15] The high flexibility in the chemical design of polymersomes allows the formation of membranes with tunable permeability responding to external stimuli, such as pH, temperature, ionic strength and electric field, through reversible structural transitions and self-adjustment of physicochemical properties.[12−15] Recently, the permeability of membrane was further fine-tuned by photocross-linking and controlled by shear-rate,[16] or by the incorporation of active molecular transporters such as transmembrane proteins.[9,17] However, in comparison to the semipermeable cellular membrane with a thickness of around 5−6 nm which is composed of low molecular weight phospholipids,[18] the permeability, fluidity, and bendability of the bilayer polymersome membrane, which is mostly composed of amphiphilic block copolymers, are still far from being satisfactory.

Recently, polymer nanocapsules[17,19−32] have attracted great interest. Some of them

* Address correspondence to huangxincn2008@yahoo.com, applhans@ipfdd.de.

Received for review July 16, 2012 and accepted October 26, 2012.

Published online October 26, 2012
10.1021/nn3031723

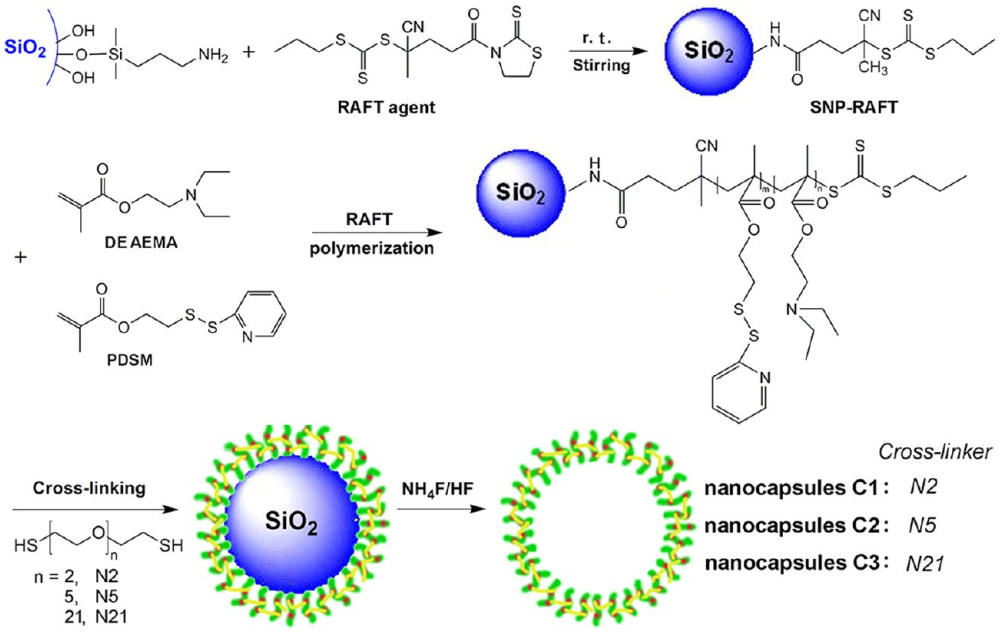

Scheme 1. The general procedure for the synthesis of polymer nanocapsules with different lengths of cross-linkers.

can be considered as polymersome-like structures, but are prepared by surface-initiated controlled radical polymerization using sacrificial nanoparticles as templates.[33−38] One of the main advantages for that approach is that the membrane can be constructed by a single polymer layer regardless of the amphiphilicity of the polymer.[35] In contrast to the bilayer membrane composed of amphiphilic block copolymer in polymersome, the single layer membrane in polymer nanocapsules seems rather interesting due to the increasing possibility to create polymer nanocapsules with ultrathin membrane and improved permeability and fluidity. More importantly, this enhanced permeability of the membrane will enlarge the size range of substances that can be postloaded in nanocapsules through the diffusion method. Thus, this provides a good platform for the potential application of highly permeable nanocapsules as nanocarrier or nanoreactor. However, so far, few reports were presented on this point. Herein, we present a new route to synthesize an intelligent polymer nanocapsule with an ultrathin membrane based on surface-initiated reversible addition−fragmentation chain-transfer (RAFT) polymerization. The key concept of our report is to use pH-responsive polydiethylaminoethylmethacrylate (PDEAEMA) as the main membrane-generating component and a degradable disulfide bond to cross-link the membrane. We aim to give a detailed study on the double tunable size of the polymer nanocapsules and membrane permeability by both pH and the length of cross-linkers. The concept was further expanded to a pH-dependent degradation by reductive glutathione (GSH) of the polymer nanocapsules, due to the modulated permeability of the membrane.

In our previous work and other reports,[33−41] it has been demonstrated that surface-initiated controlled radical polymerization with a sacrificial nanoparticle as template is an efficient method to synthesize polymer nanocapsules with controllable abilities and properties. Thus, one can well control the size of the nanocapsule and the thickness and composition of the membrane, for example, by choosing different size templates, varying the molecular weight of the polymer or using different functional monomers. At present, with the rapid development of polymer chemistry,[42−45] more and more diversity of structural and functional properties of polymers were reported which gives a good foundation for creating various functionalized polymer nanocapsules for different purposes. Without doubt this method will become one of the most robust strategies to construct polymer nanocapsules.

RESULTS AND DISCUSSION

In this report, we developed the method of surface-initiated RAFT polymerization with silica nanoparticles (SNP) as templates to synthesize an intelligent polymer nanocapsule. The procedure is summarized in Scheme 1. First, to realize controlled polymerization of the pH sensitive monomer diethylaminoethyl methacrylate (DEAEMA), a trithiol RAFT agent thioazoline active ester was newly synthesized and anchored on the surface of silica nanoparticles (SNP-RAFT). The successful anchoring of the trithiol RAFT agent onto SNP was confirmed by FT-IR, TGA, and XPS (Figure S5, S6 and XPS study in the Supporting Information (SI)). From the TGA, the

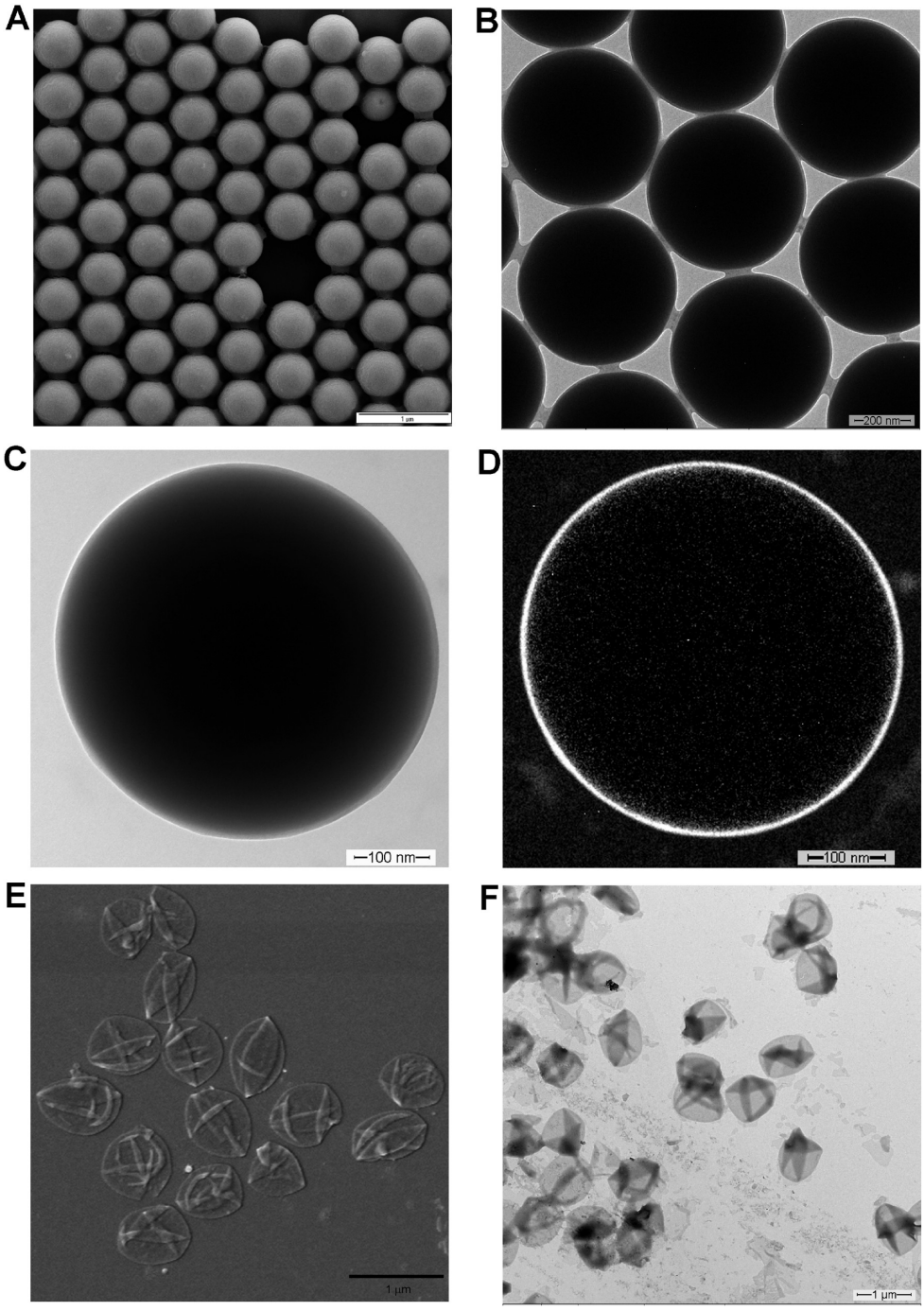

Figure 1. (A) SEM, (B) TEM, (C) magnified TEM, and (D) carbon map derived form energy filtered TEM images of PDEAEMA-*co*-PPDSM grafted SNP (M_n of the grafted copolymer, 14500 g/mol; PDI, 1.23 by GPC), (E) SEM and (F) TEM images of PDEAEMA-*co*-PPDSM nanocapsules (silica nanoparticles were dissolved with NH_4/HF buffer for panels E and F).

density of the RAFT agent on the particle surface was calculated to be 12 μmol per gram of SNP-RAFT. Second, the monomer pyridyldisulfide ethylmethacrylate (PDSM) was synthesized from commercially available aldrithiol-2 in two steps (see SI for the synthesis route). It is known that the pyridyl disulfide moiety in the monomer can be exchanged in high yields by reacting with a thiol compound of interest. Here, it is used to react with a dithiol cross-linker to stabilize the nanocapsule structures after removing the silica core. Lastly, using SNP-RAFT as a RAFT agent and DEAEMA and PDSM as monomers, surface-initiated RAFT polymerization proceeded and gave a core–shell structure with the copolymer PDEAEMA-*co*-PPDSM as the shell (SNP-polymer). FT-IR, TGA, and XPS confirmed well that the polymerization takes place on the surface. Strong evidence is, for example, the stretching vibration of ester carbonyl group in PDEAEMA chain at

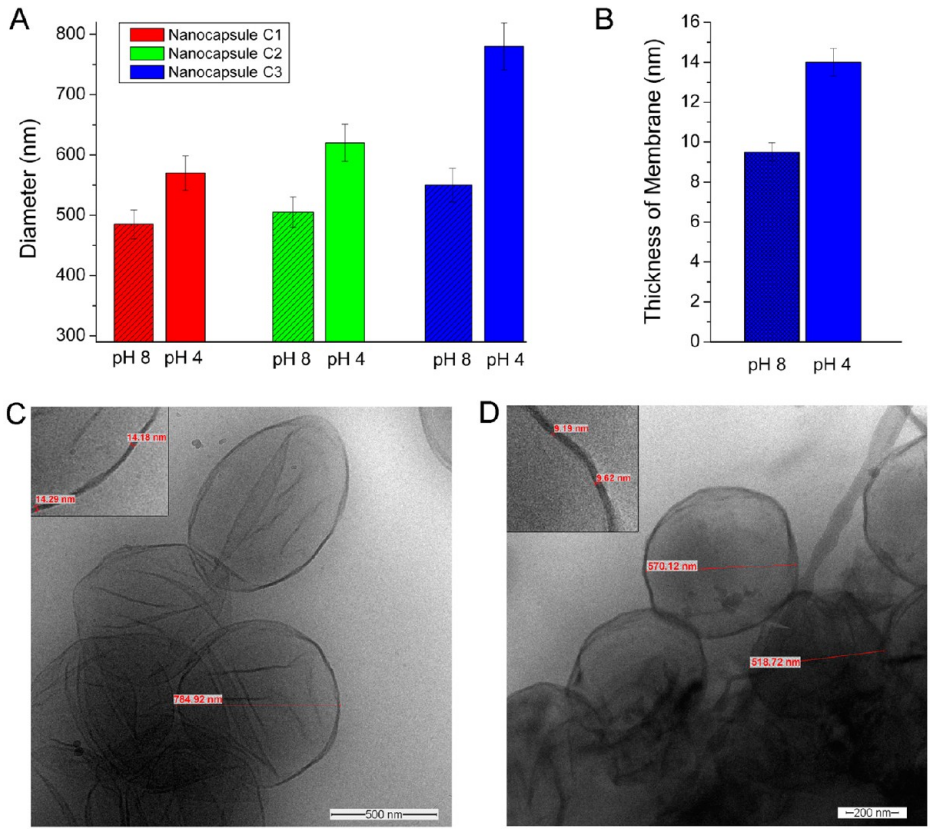

Figure 2. (A) Diameter of nanocapsules C1 to C3 in pH 4.0 and 8.0 buffer solution, respectively, measured by DLS; (B) thickness of the membrane of nanocapsules C3 at pH 4.0 and pH 8.0; (C and D) cryo-TEM images of nanocapsules C3 in pH 4.0 and pH 8.0 solution. (The error bars in Figure 2A are based on three repeated measurement, and those in Figure 2B are based on measuring three different shell areas).

1735 cm^{-1} and the obvious enhancement of the methyl signal at 2970 cm^{-1} in the IR spectrum (Figure S5, SI); the increasing intensity of S 2p peak in XPS spectrum and enhanced molar ratio of [S]:[C] (Figure S13, SI); and the additional 5% weight loss compared with the precursor SNP-RAFT in TGA (Figure S6, SI). Also, after dissolution of the silica core without cross-linking the polymer shell in advance, the isolated originally grafted copolymer was subjected to characterization by ^1H NMR (Figure S7, SI) and GPC. The number-average molecular weight of the grafted copolymer prepared in this study has been shown to be about 14500 g/mol with the molar ratio of the repeating unit of DEAEMA/PDSM at about 4/1. Moreover, the formation of this core shell structure is observed by SEM and TEM (Figure 1 A and B). The magnified image, presented in Figure 1C, clearly shows a very uniform polymer shell with a thickness of about 8.5 nm formed around the particle. Furthermore, this shell was more clearly demonstrated by carbon mapping using energy filtered TEM (Figure 1D), where the shell appears as a white ring.

To obtain stable polymer nanocapsules by the described approach, cross-linking of the shell is absolutely necessary. Here, we first used 2,2′-(ethylenedioxy)diethanethiol (N2) as the cross-linker. The progress of the cross-linking reaction, in which the disulfide bridge of the PDSM monomer is replaced by a disulfide bridge formed by the dithiol, was monitored by recording UV absorption spectroscopy of the released 2-pyridinethione ($\lambda_{max} = 375$ nm) (Figure S8, SI). Then, the silica core was removed using NH_4F/HF buffer to give the polymer nanocapsules (nanocapsules C1). SEM and TEM images (Figure 1E and F) clearly demonstrate the formation of the hollow nanocapsules structure with a size of about 520 nm. The collapsed nanocapsules structures in the images (Figure 1E and F) occur because the thin cross-linked polymer shell is not stable enough to remain a spherical structure in the dried state.

Subsequently, the controllable permeability of the synthesized polymer nanocapsules was investigated. To demonstrate the double tunable permeability by pH and the length of cross-linkers, first trials were directed to the easy pH modulation of the membrane permeability. This is caused by the fact that the PDEAEMA chain in the membrane undergoes physicochemical changes going from an unprotonated, hydrophobic entangled state at a high pH value to a protonated, hydrated, repulsive state at a low pH value. The switching of the membrane from unprotonated into protonated state is directly observable by the change in the size of nanocapsules when applying DLS measurements. The data obtained from DLS are summarized in Figure 2A. For example, investigating

nanocapsules C1 with the shortest cross-linker N2, there is an about 20% increase in diameter when the pH is changed from 8.0 to 4.0, with the change of zeta potential from 3.7 mV at pH 8.0 to 37.3 mV at pH 4.0. However, considering the potential application of the nanocapsules as nanocarrier, nanoreactor, or drug delivery vehicle which need to encapsulate larger compounds, the fine modulation of the membrane permeability by pH is still not satisfying and needs to be optimized. Therefore, to widen the tuning capacity of the membrane permeability, three different lengths of the dithiol cross-linkers (N2, N5, and N21) were employed, and the synthesized nanocapsules were noted accordingly as nanocapsules C1, C2, and C3 (Scheme 1). These three nanocapsules are synthesized under the same conditions and using the same batch of core shell particles as precursors. Thus, the only difference is the length of cross-linker. As it is expected, comparing the diameter of nanocapsules C1 with the shortest cross-linker N2 and nanocapsules C3 with the longest cross-linker N21 at pH 4.0, one can see an obvious increase from 570 nm for nanocapsules C1 up to 780 nm for nanocapsules C3, whereas the differences in capsule dimensions at pH = 8.0 are much lower (between 480 and 560 nm) (Figure 2A). This impressively shows the tailoring capacity of the combination of two adjusting factors, pH and the length of cross-linker, in this study for the fabrication polymeric nanocapsules having high difference in swelling capacity. Such a dramatic change in diameter of the nanocapsules based on identical surface grafted templates (varying from the smallest nanocapsules C1 (480 nm, at pH 8.0) up to the biggest nanocapsules C3 (780 nm, at pH 4.0) has to be emphasized, since the change of diameter of the nanocapsules will be accompanied by the change of pore size in the membrane. This may allow for encapsulating relatively big substances, such as small proteins into the nanocapsules. Moreover, to further confirm the morphology of the nanocapsules in solution, cryo-TEM was employed. As shown in Figure 2C and 2D, an extended and shrunken status of nanocapsules C3 are present in acidic and basic solution, respectively. Also, the change in thickness of the membrane against pH was observed directly from the magnified images (Figure 2B, and the inset in Figure 2C and D). The results imply that the thickness of the membrane varies from 9.5 nm in basic solution to 14 nm in acidic solution. Additionally, it is worth noting that the more creased morphology of the nanocapsules in acidic solution (Figure 2C) indicates that the well extended polymer chains of the nanocapsule leads to a membrane with features similar to that of a cellular membrane which should lead to a good fluidity and bendability.

To evaluate the real permeability of the nanocapsules, the membrane traffic was accordingly tested by using molecules in different sizes: Rhodamine B and maltose-decorated hyperbranched poly(ethylene imine) (PEI-Mal) nanoparticles[46] with PEI cores of 5000 Da (PEI-Mal 5, 5 nm) and 25 000 Da (PEI-Mal 25, 11 nm). The latter two macromolecules are chosen considering that they possess protein-sized and soft structures. To monitor the membrane traffic of PEI-Mal 5 and 25 effectively by UV spectrum, the two PEI-Mal macromolecules were labeled by fluorescein isothiocyanate (FITC). For evaluating the permeability of nanocapsuleś membrane, after mixing the solution of the chosen (macro-)molecule with the swollen nanocapsules C1, C2, or C3 at pH 4.0, and removing the free (macro-)molecule at pH 8.0 by dialysis from the shrunken nanocapsules, the remaining nanocapsule solution was analyzed by UV spectroscopy. The diffusion results are summarized in Table 1 and Figure S10 (SI). The small molecule Rodamine B can enter all of the three nanocapsules, while the bigger macromolecule PEI-Mal 5 can only enter nanocapsules C3 with a loading capacity of about 6.6 μg of PEI-Mal 5 *per* milligram of nanocapsules C3. Furthermore, the biggest macromolecule PEI-Mal 25 cannot enter any nanocapsules. Taking into account the increased pore size in the swollen membrane from the nanocapsules C1 to C3, these diffusion results are understandable when knowing that the swollen membrane in all nanocapsules is cationic. Then it is more explainable why the larger cationic PEI-Mal 25 will not be uptaken inside of the largest nanocapsule C3. The size of the successfully enclosed PEI-Mal 5 (5 nm) which is on the same level as some proteins or enzymes, thus, the permeability capacity of nanocapsules C3 can be considered very useful with the potential to be a vehicle for transporting proteins or to be a nanoreactor after loading differently charged enzymes inside the core.

TABLE 1. Permeability of the Nanocapsules against Different Substances at pH 4.0

	Rhodamine B	PEI-Mal 5-FITC[b] (M_w of PEI 5000)	PEI-Mal 25-FITC[b] (M_w of PEI 25000)
nanocapsules C1[a]	yes[c]	no	no
nanocapsules C2	yes	no	no
nanocapsules C3	yes	yes[d]	no

[a] The synthesized polymer nanocapsules with different cross-linkers (Scheme 1). [b] The diameter of PEI-Mal 5-FITC and PEI-Mal 25-FITC are 5 and 11 nm, respectively. [c] The loading capacity is about 0.13 mg of rhodamine B *per* milligram of nanocapsules C1. [d] The loading capacity is about 6.6 μg of PEI-Mal 5 *per* milligram of nanocapsules C3.

In a further study, pH-dependent degradability of the nanocapsules was shown using reductive glutathione (GSH) to cleave the disulfide bonds. Nanocapsules C3 were used as an example to study the change on diameter of nanocapsules against time at pH 4.0 and pH 8.0 in the presence of GSH, monitored by DLS (Figure 3D). As expected, at pH 4.0 it takes a shorter time to completely degrade the capsules than at pH 8.0. This pH-dependent degradability behavior is an indirect response to the pH-controlled permeability of

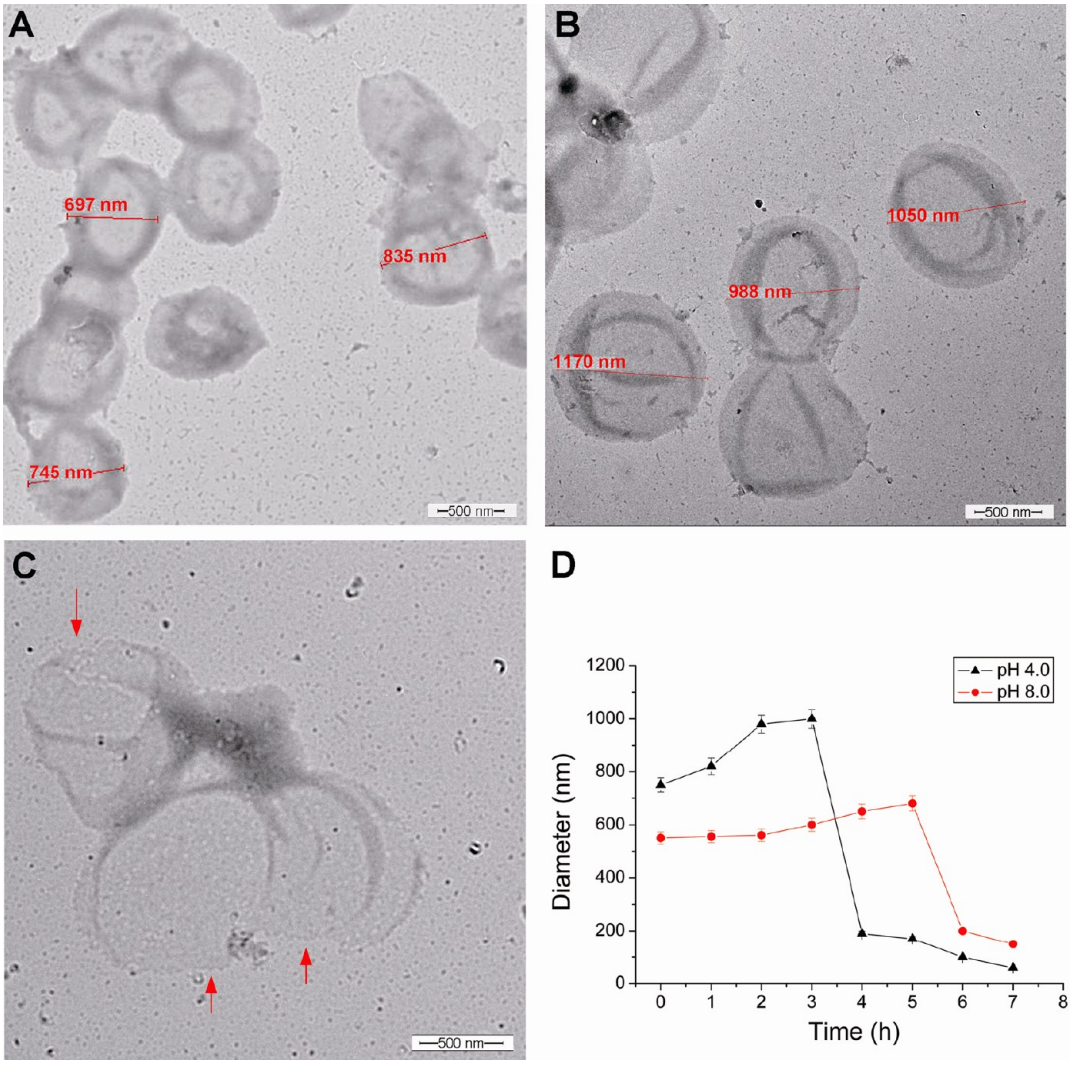

Figure 3. TEM images (A–C) show nanocapsules of C3 after adding GSH (25 mM) at pH 4.0 buffer solution for 1, 2, and 3 h, respectively, (D) the change of diameter of nanocapsules C3 at pH 4.0 (red) and pH 8.0 (black) against time after adding GSH (25 mM). (The error bars in Figure 3D were based on three repeated measurements.)

the membrane. In acidic solution, the opened membrane of the nanocapsules allows for GSH to easily approach the disulfide bonds accelerating the disassembly of the nanocapsules. Conversely, in basic solution, the tightly aggregated membrane of the nanocapsules hinders GSH to approach the disulfide bonds and slows down the degradation of the nanocapsules. Interestingly, from the curve Figure 3D it can be seen that after adding GSH the diameter of nanocapsules goes up first, then goes down. This mainly occurs at the beginning of degrading, the partial cleavage of disulfide bonds results in a swelling of the nanocapsules. Then, with the reaction proceeding, more disulfide bonds are reduced which leads to the disassembly of the nanocapsules. TEM was employed to observe the different morphology states at different degrading times in acidic solution against GSH (Figure 3A–C). From Figure 3A (1 h) and Figure 3B (2 h), one can see an obvious increase in diameter by the comparison with that before adding GSH (around 700 nm), and a seriously destroyed morphology is seen in Figure 3C after 3 h GSH treatment. The totally disassembled morphology of nanocapsules C3 is also shown in Figure S11 (SI) after 6 h reaction. In view of the increased concentration of GSH and the relative acidic environment in some cancer tumors, the pH-dependent degradability bestows nanocapsules another virtue. Applying those nanocapsules as a nanocarrier in drug delivery, degradable nanocapsules will give a burst-release to the cancer cells, once taken up in those cells. Furthermore, the mild reducing agent ascorbic acid has also been employed to investigate this degradability, but from DLS data under the concentration of 25 mM of ascorbic acid, we could observe that the polymer nanocapsules C2 cannot be completely destroyed within 24 h (Figure S12, SI).

Finally, to further demonstrate the potential application of this polymer nanocapsule as a nanoreactor, an enzyme, myoglobin, was incorporated inside the hollow core. Myoglobin is an iron-containing protein with

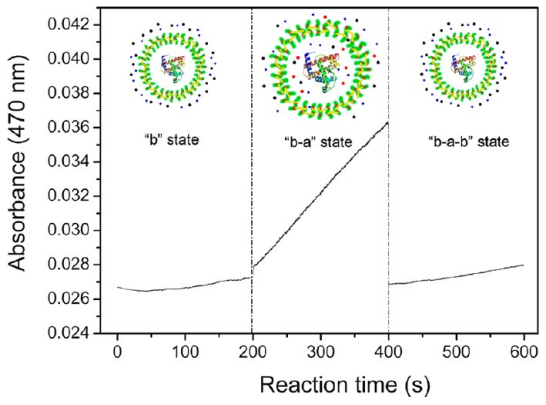

Figure 4. Schematic representation of the reaction of guaiacol and hydrogen peroxide in myoglobin-filled nanocapsules C3 with longest cross-linker N21: first the catalyzing reaction was in a basic solution of pH 8.0 ("b" state), then the pH of the reaction solution was adjusted to 6.0 ("b−a" state), and last pH of the reaction solution was adjusted back to 8.0 again ("b−a−b" state). For each state the reaction was monitored by recording UV absorbance at 470 nm for 200 s.

the size about 3.1 × 3.4 × 6.4 nm^3,[47] and able to catalyze oxidative reactions of guaiacol with hydrogen peroxide as a substrate. Since it has been shown that PEI-Mal 5-FITC (5 nm) can be encapsulated by nanocapsules C3, this nanocapsule was also employed as the enzyme carrier. Myoglobin was loaded into polymer nanocapsules C3 at pH 4.0, then the unloaded myoglobin was removed by dialysis with PBS buffer at pH 8.0. Subsequently, this myoglobin-filled nanocapsule solution was subjected to an enzymatic activity test at different pH states (Figure 4). The first measurement showed that at pH 8.0 a very low activity was observed in the presence of guaiacol and hydrogen peroxide as substrates (Figure 4, "b" state). Since at this pH value, the PDEAEM membrane is unprotonated and fully hydrophobic, the hydrophilic hydrogen peroxide cannot easily diffuse through the hydrophobic membrane to reach the encapsulated myoglobin in the core which results in the low activity. However, after adjusting the pH value of the measured solution to pH 6.0, an obviously enhanced activity was observed (Figure 4, "b−a" state). This is because the nanocapsule membrane is now in a swollen state and totally hydrophilic which makes the transmembrane diffusion possible, thereby allowing the guaiacol and hydrogen peroxide to reach the myoglobin in the core and accelerate the reaction. When the pH value is adjusted back to 8.0, as expected, the reaction becomes again slow because the nonpermeable membrane reforms (Figure 4, "b−a−b" state). Here, we found a similar behavior of the nanocapsules membrane as previously described for our pH-sensitive and photocross-linked membrane in pH-stable polymersomes.[16]

CONCLUSION

In this study, intelligent polymer nanocapsules were synthesized by using a surface-initiated RAFT polymerization technique on silica templates and the pH sensitive monomer DEAEMA as well as the disulfide containing monomer PDSM as main units. Cross-linking was successfully achieved by different lengths dithiols and led to stable nanocapsules after removal of the silica template. The fabrication of the nanocapsules structures were confirmed well by IR, TGA, ^{1}H NMR, GPC, XPS, SEM, and cryo-TEM. The permeability of membrane could be well tuned by adjusting the pH and using different lengths of the cross-linkers. Also, due to the disulfide cross-linker, degradation of the capsules using GSH as reducing agent can be achieved which is further significantly promoted at pH 4.0. Using a rather long-chain dithiol cross-linker it could be demonstrated that the protein-sized and cationic macromolecule PEI-Mal 5-FITC can successfully go through the cationic membrane in the swollen state which makes this nanocapsule to be a very promising candidate in the application as nanoreactors or nanocarriers. This was even demonstrated by a first model of postencapsulation of the cationic enzyme myoglobin at pH 4.0 and showing pH controlled enzyme activity by switching membrane permeability between pH 6.0 and 8.0. Thus it could be demonstrated that surface-initiated controlled radical polymerization of functional monomers followed by intelligent cross-linking strategies before removing the template is a robust approach to construct well-defined smart polymer nanocapsules. It is foreseeable that with the rapid development of polymer chemistry, the high diversity of structural and functional polymer nanocapsules accessibility will allow for studying complex transmembrane transport in biology and will also enrich nanoreactors or carrier system for tuning the polymeric membrane composition to more adapt biological membrane features.

EXPERIMENTAL SECTION

Synthesis of Mercaptothiazoline Activated 4,4′-Azobis(4-cyanovaleric acid) (ACVA−ACPM). (The general synthesis procedure was shown in Scheme S1, in SI). A solution of 4,4′-azobis(4-cyanovaleric acid) (ACVA, 4.01 g, 14.3 mmol) and 2-mercaptothiazoline (4.50 g, 37.8 mmol) in 1,4-dioxane (200 mL) was degassed by nitrogen for 30 min. *N*,*N*′-Dicyclohexylcarbodiimide (DCC, 6.82 g, 33.0 mmol) and 4-(dimethylamino)pyridine (DMAP, 0.10 g, 0.82 mmol) dissolved in 1,4-dioxane (100 mL) were added slowly at room temperature under rigorous stirring. After 20 h, the reaction mixture was filtered and concentrated. The product was precipitated in cold diethyl ether. After being dried under vacuum, ACVA-ACPM was obtained as a yellow powder (5.96 g, 86.3% yield). ^{1}H NMR (500 MHz, $CDCl_3$): d (ppm) 4.59 (t, 2H, NCH_2CH_2S), 3.31 (t, 2H, NCH_2CH_2S), 3.15−3.62 (m, 2H, $(CN)C(CH_3)CH_2CH_2CON$), 2.42−2.64 (m, 2H, $(CN)C(CH_3)CH_2CH_2CON$), 1.76 (s, 3H, $(CN)C(CH_3)CH_2$).

^{13}C NMR (125 MHz, $CDCl_3$): d (ppm) 201.9 (NC═S), 172.0 (CH2CON), 117.5 ($(CH_3)C(CN)CH_2$), 72.0, 56.0, 34.0, 32.9, 28.4, 24.2.

Synthesis of Bis(propylsulfanylthiocarbonyl) Disulfide. Propanethiol (5.79 g, 76 mmol) was added over 10 min to a stirred suspension of sodium hydride (60% in oil) (3.15 g, 79 mmol) in diethyl ether (150 mL) at 0 °C. The solution was then allowed to stir for 10 min prior to the addition of carbon disulfide (6.0 g, 79 mmol). Crude sodium *S*-propyl trithiocarbonate (7.85 g, 0.049 mol) was collected by filtration, suspended in diethyl ether (100 mL), and reacted with iodine (6.3 g, 0.025 mol). After 1 h the solution was filtered, washed with aqueous sodium thiosulfate, and dried over sodium sulfate. The crude bis(propylsulfanylthiocarbonyl) disulfide was then isolated by rotary evaporation.

Synthesis of Mercaptothiazoline Activated Trithiol-RAFT Agent 4-Cyano-4-(ethylsulfanylthiocarbonyl) Sulfanylpentanoic Acid Mercaptothiazoline Ester. A solution of bis(ethylsulfanylthiocarbonyl) disulfide (1.37 g, 0.005 mol) and ACVA-ACPM (3.0 g, 0.0075 mol) in ethyl acetate (50 mL) was heated at reflux for 18 h. Following rotary evaporation of the solvent, the crude product was isolated by column chromatography using silica gel as the stationary phase and 50:50 ethyl acetate/*n*-hexane as the eluent. ^{1}H NMR and ^{13}C NMR were shown in the SI, Figure S1 and S2.

Synthesis of Compound Pyridyldisulfide Ethanol. (The general synthesis procedure was shown in Scheme S2, in SI). Aldrithiol-2 (15g, 0.068 mol) was dissolved in 75 mL of methanol, and 1 mL of glacial acetic acid was added to it. To this mixture, a solution of mercaptoethanol (2.65 g, 33.97 mmol) in 15 mL of methanol was added dropwise at room temperature with continuous stirring. Once the addition was over, the reaction mixture was stirred at room temperature for an additional 3 h. Then the solvent was evaporated to get the crude product as a yellow oil which was purified by flash column chromatography using silica gel as a stationary phase and a mixture of ethyl acetate/hexane as eluent. The excess aldrithiol came out first at 15% ethyl acetate/*n*-hexane mixture, then the polarity of the eluent was increased to 40% ethyl acetate/*n*-hexane to get the desired product as a colorless oil. Yield, 52%.

Synthesis of Monomer Pyridyldisulfide Ethylmethacrylate (PDSM). To a solution of compound 8 (4.62 g, 24.7 mmol) in 20 mL of dry dichloromethane was added 3 g (29.7 mmol) of triethylamine, and the mixture was cooled in an ice-bath. To this cold mixture, a solution of purified methacryloyl chloride (2.58 g, 24.7 mmol) in 10 mL of dichloromethane was added dropwise with continuous stirring. After the addition was over, the reaction mixture was stirred at room temperature for 6 h. The stirring was stopped and the reaction mixture was washed with 3 × 30 mL of distilled water and then with 30 mL of brine. The organic layer was collected, dried over anhydrous Na_2SO_4 and concentrated to get the crude product as a yellow oil. It was purified by column chromatography using silica gel as the stationary phase and a mixture of ethyl acetate/hexane as eluent. The pure product was collected at 25% ethylacetate/hexane (yield: 71%). ^{1}H NMR and ^{13}C NMR were shown in SI, Figure S3 and S4.

Preparation of Amino-Functionalized SNP. Smooth and monodisperse SNPs were synthesized according to the Stöber method.[48] Then a suspension (16 mL) of 10 wt % SNP was added to a round-bottom flask with 3-aminopropyldimethylethoxysilane (1.0 g, 6.0 mmol) and ammonium hydroxide solution (1 mL, 16 mmol). The reaction mixture was stirred at room temperature for 20 h. The particles were obtained by centrifugation of the reaction mixture at 3000 rpm for 5 min. Then the particles were thoroughly washed *via* centrifugation/redispersion cycles with ethanol for five times. The amino-functionalized SNP was dispersed directly into 50 mL of THF for subsequent use. An aliquot of the amino-functionalized SNP was dried and subjected to thermal gravimetric analysis (TGA) and XPS study (in SI).

Preparation of RAFT Agent Anchored Silica Nanoparticles. A THF solution of the amino-functionalized silica nanoparticles (25 mL, 4.0%) was added dropwise to a THF solution (30 mL) of R-group activated RAFT agent (378 mg, 1.0 mmol) at room temperature. After complete addition, the solution was stirred for another 6 h. The particles were recovered by centrifugation of the reaction mixture at 3000 rpm for 5 min followed by washing the particles with THF at least 5 times until the supernatant layer was colorless after centrifugation. Finally, the RAFT agent anchored silica nanoparticles were dispersed in 1,4-dioxane for subsequent use.

RAFT Polymerization Based on the RAFT Agent Anchored SNP. RAFT agent anchored SNP (30 mg, 10 μmol RAFT/g), 4-cyano-4-(ethylsulfanylthiocarbonyl) sulfanylpentanoic acid (4.5 mg, 16.2 μmol), DMF (3 mL), DEAEMA (400 mg, 2.81 mmol), and PDSM (160 mg, 0.63 mmol) were added to a 10 mL round-bottom flask followed by sonication and addition of V-70 (0.98 mg, 3.2 μmol). The flask was sealed and the solution was purged with argon for 30 min in an ice bath before heating to 35 °C. After 15 h (conversion 40%), the solution was centrifuged and the particles were collected. The cycle of centrifugation and redispersion in THF was repeated at least five times to ensure no free polymer remaining on the SNP surface. The product was dried *in vacuo* to yield a pink powder. After removal of the silica core with NH_4F/HF buffer, the obtained grafted polymer was characterized by ^{1}H NMR and GPC.

Preparation of Hollow Nanocapsules. After the polymerization mentioned above, the core−shell structures were isolated from the solvent by centrifugation (30 mg) and placed in a 10 mL flask with 4 mL of ethanol. The solution was sonicated for 30 min before adding dithiol cross-linker to cross-link the shell. After stirring for 4 h, the particles were recovered by centrifugation at 3000 rpm for 5 min. Then the inorganic silica core was etched by 8 M NH_4F/2 M HF buffer (pH ≈ 5): briefly, 30 mg of the copolymer grafted SNP was stirred in 2 mL of NH_4F/HF buffer at room temperature for 12 h to dissolve the silica core. (Caution: HF is hazardous and very corrosive. Goggles and gloves must be worn during the operation.) The excess NH_4F, HF, and SiF_4 were removed from hollow nanospheres by dialysis in deionized water for 3 days. Finally, the hollow nanocapsules can be obtained by a freeze-drying process.

Conflict of Interest: The authors declare no competing financial interest.

Acknowledgment. X. Huang is grateful for the fellowship from the Alexander von Humboldt Foundation. The authors also would like to thank Maria Auf der Landwehr, Hartmut Komber, Jens Gaitzsch, Liane Häussler, Anja Caspari, and Mikhail Malanin for their help with SEM, NMR, GPC, TGA, DLS, and FTIR, and all other colleagues who contributed to the work.

Supporting Information Available: Materials and instruments used in this study, and characterization of the RAFT agent and polymer nanocapsules, ^{1}H NMR, ^{13}C NMR, FT-IR, UV, TGA, and XPS study. This material is available free of charge *via* the Internet at http://pubs.acs.org.

REFERENCES AND NOTES

1. Mann, S. Systems of Creation: The Emergence of Life from Nonliving Matter. *Acc. Chem. Res.* **2012**, 10.1021/ar200281t.
2. Szostak, J. W.; Bartel, D. P.; Luisi, P. L. Synthesizing Life. *Nature* **2001**, *409*, 387–390.
3. Zelikin, A. N.; Price, A. D.; Städler, B. Poly (methacrylic acid) Polymer Hydrogel Capsules: Drug Carriers, Sub-compartmentalized Microreactors, Artificial Organelles. *Small* **2010**, *6*, 2201–2207.
4. Discher, B. M.; Won, Y. Y.; Ege, D. S.; Lee, J. C. M.; Bates, F. S.; Discher, D. E.; Hammer, D. A. Polymersomes: Tough Vesicles Made from Diblock Copolymers. *Science* **1999**, *284*, 1143–1146.
5. Discher, D. E.; Eisenberg, A. Polymer Vesicles. *Science* **2002**, *297*, 967–973.
6. Lomas, H.; Canton, I.; MacNeil, S.; Du, J.; Armes, S. P.; Ryan, A. J.; Lewis, A. L.; Battaglia, G. Biomimetic pH Sensitive Polymersomes for Efficient DNA Encapsulation and Delivery. *Adv. Mater.* **2007**, *19*, 4238–4243.
7. Jaskiewicz, K.; Larsen, A.; Lieberwirth, I.; Koynov, K.; Meier, W.; Fytas, G.; Kroeger, A.; Landfester, K. Probing Bioinspired Transport of Nanoparticles into Polymersomes. *Angew. Chem., Int. Ed.* **2012**, *51*, 4613–4617.
8. van Dongen, S. F. M.; de Hoog, H. P. M.; Peters, R. J. R. W.; Nallani, M.; Nolte, R. J. M.; van Hest, J. C. M. Biohybrid Polymer Capsules. *Chem. Rev.* **2009**, *109*, 6212–6274.

9. Renggli, K.; Baumann, P.; Langowska, K.; Onaca, O.; Bruns, N.; Meier, W. Selective and Responsive Nanoreactors. *Adv. Funct. Mater.* **2011**, *21*, 1241–1259.
10. Kim, K. T.; Cornelissen, J. J. L. M.; Nolte, R. J. M.; van Hest, J. A Polymersome Nanoreactor with Controllable Permeability Induced by Stimuli-Responsive Block Copolymers. *Adv. Mater.* **2009**, *21*, 2787–2791.
11. Christian, D. A.; Cai, S.; Bowen, D. M.; Kim, Y.; Pajerowski, J. D.; Discher, D. E. Polymersome Carriers: from Self-assembly to siRNA and Protein Therapeutics. *Eur. J. Pharm. Biopharm.* **2009**, *71*, 463–474.
12. Carlsen, A.; Glaser, N.; Le Meins, J. F.; Lecommandoux, S. Block Copolymer Vesicle Permeability Measured by Osmotic Swelling and Shrinking. *Langmuir* **2011**, *27*, 4884–4890.
13. Le Meins, J. F.; Sandre, O.; Lecommandoux, S. Recent Trends in the Tuning of Polymersomes' Membrane Properties. *Eur. Phys. J., E: Soft Matter Biol. Phys.* **2011**, *34*, 1–17.
14. Kim, M. S.; Lee, D. S. Biodegradable and pH-Sensitive Polymersome with Tuning Permeable Membrane for Drug Delivery Carrier. *Chem. Commun.* **2010**, *46*, 4481–4483.
15. Kim, K. T.; Zhu, J.; Meeuwissen, S. A.; Cornelissen, J. J. L. M.; Pochan, D. J.; Nolte, R. J. M.; van Hest, J. C. M. Polymersome Stomatocytes: Controlled Shape Transformation in Polymer Vesicles. *J. Am. Chem. Soc.* **2010**, *132*, 12522–12524.
16. Gaitzsch, J.; Appelhans, D.; Wang, L.; Battaglia, G.; Voit, B. Synthetic Bio-nanoreactor: Mechanical and Chemical Control of Polymersome Membrane Permeability. *Angew. Chem., Int. Ed.* **2012**, *51*, 4448–4451.
17. Brinkhuis, R. P.; Rutjes, F. P. J. T.; van Hest, J. C. M. Polymeric Vesicles in Biomedical Applications. *Polym. Chem.* **2011**, *2*, 1449–1462.
18. Rawicz, W.; Olbrich, K.; McIntosh, T.; Needham, D.; Evans, E. Effect of Chain Length and Unsaturation on Elasticity of Lipid Bilayers. *Biophys. J.* **2000**, *79*, 328–339.
19. Caruso, F.; Caruso, R. A.; Möhwald, H. Nanoengineering of Inorganic and Hybrid Hollow Spheres by Colloidal Templating. *Science* **1998**, *282*, 1111–1114.
20. Bédard, M. F.; De Geest, B. G.; Skirtach, A. G.; Möhwald, H.; Sukhorukov, G. B. Polymeric Microcapsules with Light Responsive Properties for Encapsulation and Release. *Adv. Colloid Interface Sci.* **2010**, *158*, 2–14.
21. Limer, A.; Gayet, F.; Jagielski, N.; Heming, A.; Shirley, I.; Haddleton, D. M. Synthesis of Microcapsules *via* Reactive Surfactants. *Soft Matter* **2011**, *7*, 5408–5416.
22. Städler, B.; Price, A. D.; Zelikin, A. N. A Critical Look at Multilayered Polymer Capsules in Biomedicine: Drug Carriers, Artificial Organelles, and Cell Mimics. *Adv. Funct. Mater.* **2011**, *21*, 14–28.
23. Li, G. L.; Tai, C. A.; Neoh, K.; Kang, E.; Yang, X. Hybrid nanorattles of Metal Core and Stimuli-Responsive Polymer Shell for Confined Catalytic Reactions. *Polym. Chem.* **2011**, *2*, 1368–1374.
24. He, W. D.; Sun, X. L.; Wan, W. M.; Pan, C. Y. Multiple Morphologies of PAA-b-PSt Assemblies throughout RAFT Dispersion Polymerization of Styrene with PAA Macro-CTA. *Macromolecules* **2011**, *44*, 3358–3365.
25. Esser-Kahn, A. P.; Odom, S. A.; Sottos, N. R.; White, S. R.; Moore, J. S. Triggered Release from Polymer Capsules. *Macromolecules* **2011**, *44*, 5539–5553.
26. Broaders, K. E.; Pastine, S. J.; Grandhe, S.; Fréchet, J. M. J. Acid-Degradable Solid-Walled Microcapsules for pH-Responsive Burst-Release Drug Delivery. *Chem. Commun.* **2011**, *47*, 665–667.
27. Ali, S. I.; Heuts, J. P. A.; van Herk, A. M. Vesicle-Templated pH-Responsive Polymeric Nanocapsules. *Soft Matter* **2011**, *7*, 5382–5390.
28. Delcea, M.; Yashchenok, A.; Videnova, K.; Kreft, O.; Möhwald, H.; Skirtach, A. G. Multicompartmental Micro- and Nanocapsules: Hierarchy and Applications in Biosciences. *Macromol. Biosci.* **2010**, *10*, 465–474.
29. Boyer, C.; Whittaker, M. R.; Nouvel, C.; Davis, T. P. Synthesis of Hollow Polymer Nanocapsules Exploiting Gold Nanoparticles as Sacrificial Templates. *Macromolecules* **2010**, *43*, 1792–1799.
30. Chong, S. F.; Lee, J. H.; Zelikin, A. N.; Caruso, F. Tuning the Permeability of Polymer Hydrogel Capsules: An Investigation of Cross-Linking Density, Membrane Thickness, and Cross-Linkers. *Langmuir* **2011**, *27*, 1724–1730.
31. Delcea, M.; Möhwald, H.; Skirtach, A. G. Stimuli-Responsive LbL Capsules and Nanoshells for Drug Delivery. *Adv. Drug Delivery Rev.* **2011**, *63*, 730–747.
32. Chen, F.; Jiang, X.; Liu, R.; Yin, J. Polymeric Vesicles with Well-Defined Poly(methyl methacrylate)(PMMA) Brushes *via* Surface-Initiated Photopolymerization (SIPP). *Polym. Chem.* **2011**, *2*, 614–618.
33. Fu, G.; Shang, Z.; Liang, H.; Kang, E.; Neoh, K. Preparation of Cross-Linked Polystyrene Hollow Nanospheres *via* Surface-Initiated Atom Transfer Radical Polymerizations. *Macromolecules* **2005**, *38*, 7867–7871.
34. Ohno, K.; Morinaga, T.; Koh, K.; Tsujii, Y.; Fukuda, T. Synthesis of Monodisperse Silica Particles Coated with Well-Defined, High-Density Polymer Brushes by Surface-Initiated Atom Transfer Radical Polymerization. *Macromolecules* **2005**, *38*, 2137–2142.
35. Blomberg, S.; Ostberg, S.; Harth, E.; Bosman, A. W.; Van Horn, B.; Hawker, C. J. Production of Crosslinked, Hollow Nanoparticles by Surface-Initiated Living Free-Radical Polymerization. *J. Polym. Sci.Part A: Polym. Chem.* **2002**, *40*, 1309–1320.
36. Morinaga, T.; Ohkura, M.; Ohno, K.; Tsujii, Y.; Fukuda, T. Monodisperse Silica Particles Grafted with Concentrated Oxetane-Carrying Polymer Brushes: Their Synthesis by Surface-Initiated Atom Transfer Radical Polymerization and Use for Fabrication of Hollow Spheres. *Macromolecules* **2007**, *40*, 1159–1164.
37. Li, G.; Liu, G.; Kang, E.; Neoh, K.; Yang, X. pH-Responsive Hollow Polymeric Microspheres and Concentric Hollow Silica Microspheres from Silica– Polymer Core– Shell Microspheres. *Langmuir* **2008**, *24*, 9050–9055.
38. Li, G.; Lei, C.; Wang, C.; Neoh, K.; Kang, E.; Yang, X. Narrowly Dispersed Double-Walled Concentric Hollow Polymeric Microspheres with Independent pH and Temperature Sensitivity. *Macromolecules* **2008**, *41*, 9487–9490.
39. Huang, X.; Appelhans, D.; Formanek, P.; Simon, F.; Voit, B. Synthesis of Well-Defined Photo-Cross-Linked Polymeric Nanocapsules by Surface-Initiated RAFT Polymerization. *Macromolecules* **2011**, *44*, 8351–8360.
40. Huang, X.; Hauptmann, N.; Appelhans, D.; Formanek, P.; Frank, S.; Kaskel, S.; Temme, A.; Voit, B. Synthesis of Heteropolymer Functionalized Nanocarriers by Combining Surface-Initiated ATRP and RAFT Polymerization. *Small* **2012**, 10.1002/smll.201201397.
41. Huang, X.; Voit, B. Progress on Multi-compartment Polymeric Capsules. *Polym. Chem.* **2012**, 10.1039/c2py20636f.
42. Matyjaszewski, K.; Tsarevsky, N. V. Nanostructured Functional Materials Prepared by Atom Transfer Radical Polymerization. *Nat. Chem.* **2009**, *1*, 276–288.
43. Boyer, C.; Stenzel, M. H.; Davis, T. P. Building Nanostructures Using RAFT Polymerization. *J. Polym. Sci.Part A: Polym. Chem.* **2011**, *49*, 551–595.
44. Boyer, C.; Bulmus, V.; Davis, T. R.; Ladmiral, V.; Liu, J. G.; Perrier, S. Bioapplications of RAFT Polymerization. *Chem. Rev.* **2009**, *109*, 5402–5436.
45. Moad, G.; Rizzardo, E.; Thang, S. H. Radical Addition–Fragmentation Chemistry in Polymer Synthesis. *Polymer* **2008**, *49*, 1079–1131.
46. Appelhans, D.; Komber, H.; Quadir, M. A.; Richter, S.; Schwarz, S.; van der Vlist, J.; Aigner, A.; Müller, M.; Loos, K.; Seidel, J.; *et al.* Hyperbranched PEI with Various Oligosaccharide Architectures: Synthesis, Characterization, ATP Complexation, and Cellular Uptake Properties. *Biomacromolecules* **2009**, *10*, 1114–1124.
47. Takano, T. Structure of Myoglobin Refined at 2.0 Å Resolution: II. Structure of Deoxymyoglobin from Sperm Whale. *J. Mol. Biol.* **1977**, *110*, 569–584.
48. Stöber, W.; Fink, A.; Bohn, E. Controlled Growth of Monodisperse Silica Spheres in the Micron Size Range. *J. Colloid Interface Sci.* **1968**, *26*, 62–69.